

A Closed-Loop Model of the Respiratory Control System

I. A. RYBAK, M. POTTMANN, B. A. OGUNNAIKE, AND J. S. SCHWABER
Advanced Process Modeling and Control Group
E. I. du Pont de Nemours and Company
Wilmington, Delaware, 19880-0101

1. Introduction

The central nervous system is capable of adjusting the rate of lung ventilation to the demands of the body so that the arterial blood composition (pH , O_2 and CO_2 tensions) is maintained within appropriate bounds even during strenuous exercise and other disturbances. A central pattern generator sends motor signals to the diaphragm to expand and contract the lungs, while it also receives feedback signals from lung stretch receptors and chemoreceptors indicating blood composition (see Figure 1). The ventilation rate, which depends on the respiratory frequency and the breathing pattern, can be considered the only manipulated variable available for satisfying several control objectives [5]. Moreover, the breathing pattern is believed to be adjusted such that the required ventilation rate is provided in the most energy-efficient manner (*ergometric minimization*) [9]. In this paper, we present a closed-loop model of the respiratory control system. In contrast to previously reported models (e.g. [2], [6], [11]), the central pattern generator is modeled on a detailed neuronal level. Moreover, we study the neural controller *in conjunction* with the periphery it controls, an approach that has not been taken with previous network models of respiratory rhythm generation (e.g. [1], [12]). Due to the interactions between the controller and the periphery it is possible to gain a better understanding of the properties of the neural control system and to guide the selection of neural network models that are physiologically plausible.

2. Respiratory rhythm generator

The basic respiratory rhythm is generated in a relatively small area of the medulla in the brainstem [5]. Typically, the neurons involved in rhythm generation are classified into several types, depending on the phase of the respiratory cycle in which they show specific bursts of activity [12]. In the present work, a network consisting of six neurons was developed

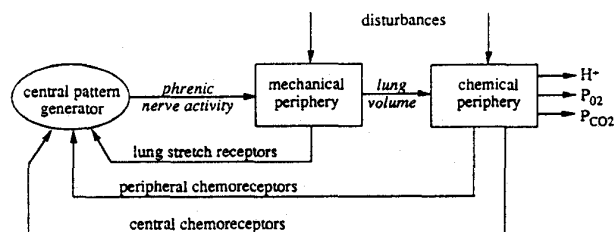


Figure 1: Schematic of the respiratory control system

to model the central pattern generator. The single-neuron model follows the classical Hodgkin-Huxley formalism using ionic channel descriptions,

$$c \frac{dU}{dt} = \sum_i g_i (E_i - U) \quad (1)$$

where c is the neuron membrane capacitance, U is the membrane potential, g_i and E_i denote the conductance and reversal potential of the i -th channel, respectively. The following channels which have been identified in each cell type are included in the model: Na^+ , several K^+ channels (delayed rectifier K_{DR} , transient K_A , calcium dependent $K_{AHP}(Ca)$) and Ca^{2+} channels (Ca_L and Ca_T), a leakage channel, as well as excitatory and inhibitory synaptic channels. Three types of neurons are employed by the rhythm generator: a basic neuron model (*type I*), as well as *type II* and *type III* neurons with adaptive and augmenting responses to constant stimuli, respectively. A complete description of the single-neuron models is given in [15]. These single-neuron properties in combination with appropriate network connections (including reciprocal inhibition) provide the switching between the individual respiratory phases.

The neural network model of the central pattern generator is shown in Figure 2, where the numbers inside the circles representing the neurons indicate the neuron type. Central to rhythm generation are

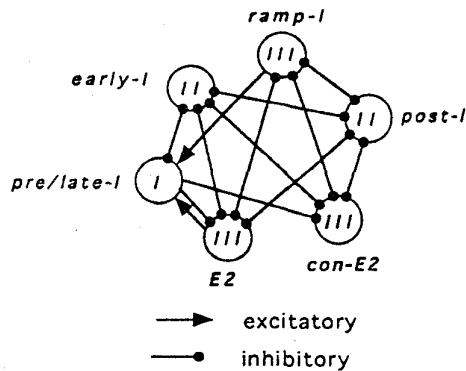


Figure 2: Model of the central rhythm generator

the switches between the respiratory phases: inspiration, post-inspiration and expiration. In the present model, the inspiratory off-switch is provided by the following mechanism [12]: The ramp-I neuron excites the pre/late-I neuron at the end of the inspiratory phase; the latter inhibits the early-I neuron, which in turn disinhibits the post-I neuron. The switch between post-inspiration and expiration emerges as a result of the reciprocal inhibition between the post-I and E2 neurons. Finally, the expiratory off-switch is provided by a mechanism very similar to the inspiratory off-switch. The pre/late-I neuron is excited by the increasing activity of the E2 neuron, and then terminates the bursts of the E2 and con-E2 neurons by strong inhibition. The E2 neuron in turn disinhibits the early-I and ramp-I neurons, thus initiating a new respiratory cycle. A detailed description of this network model for rhythm generation and comparisons with alternative network architectures are given in [14].

The output of the respiratory network is the phrenic nerve activity, which is a weighted sum of the spiking activities of the ramp-I and post-I neurons.

3. Peripheral model

The model of the respiratory periphery, which consists of a mechanical and a chemical part, is assumed to be driven by the phrenic nerve activity (see Figure 1). In the mechanical periphery, the phrenic signal is transformed into muscle movements and eventually into lung volume changes, which in turn constitute the input to the chemical periphery. The latter is modeled in the form of separate compartments for lungs, body tissue, cerebrospinal fluid and brain tissue. These compartment models are based on simplified mass balance equations [6]. The complete peripheral model is given in the Appendix.

The peripheral model is used to predict the dynamic

effects of the phrenic nerve activity and various disturbances (hypoxia, hypercapnia, hyperventilation, exercise, etc.) on the state of the respiratory periphery, which is described by variables such as lung volume, alveolar, arterial and venous CO_2 and O_2 tensions.

4. Closed-loop model

The central pattern generator receives the following types of feedback from the respiratory periphery:

Vagal feedback: Pulmonary stretch receptors (PSR) are known to play an important role in the phase switching of the central rhythm generator [3], [13]. Here it is assumed that, after a certain threshold volume has been reached, the PSR fire at a rate proportional to the lung volume [3]. Furthermore, PSR afferents inhibit the early-I neuron, and excite the post-I neuron. This PSR feedback configuration is supported by experimental studies [5] [13].

Chemical feedback: The central rhythm generator is subject to inputs from both central and peripheral chemoreceptors. Central receptors, which are located in the medulla, have the following characteristics: they are mainly responsive to CO_2 , and they respond rather slowly to blood CO_2 changes [9]. By contrast, peripheral chemoreceptors, located in the carotid bodies, transmit information on arterial blood composition very promptly. Moreover, they are also sensitive to O_2 , in particular at low O_2 levels (below 60 mm Hg) where the hemoglobin O_2 saturation with oxygen decreases rapidly [9]. The spiking frequency of peripheral chemoreceptors can thus be assumed to be a nonlinear function of CO_2 and O_2 tensions. The experimental data in [8] suggest the following functional form to approximate the peripheral chemoreceptor activity, I_p ,

$$I_p = a_0 P'_{aCO_2} [a_1 e^{-P'_{aO_2}/a_2} + 1] \quad (2)$$

where the prime (') denotes delayed values of arterial gas tensions. Thus, the peripheral chemoreceptor activity depends linearly on P'_{aCO_2} , and exponentially on P'_{aO_2} . Although chemoreceptors do not directly project onto respiratory neurons [10], we assume that these neurons receive a chemical drive signal that is directly related to chemoreceptor activity. For simplicity, the effects of central and peripheral chemoreceptors are lumped together into a single chemical drive signal, I_{ch} , according to,

$$I_{ch} = I_p + I_c \quad (3)$$

where the central chemoreceptor activity, I_c , is taken to be proportional to the CO_2 tension at the lo-

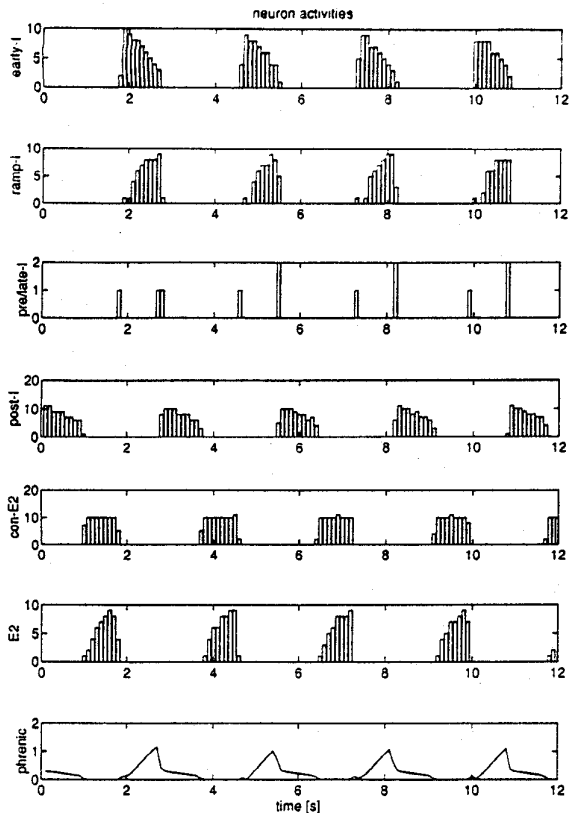


Figure 3: Nominal neuron activities

cation of the central receptors in the medulla (see the Appendix). All neurons in the respiratory network receive a drive signal, I_i , which is excitatory for every neuron except for the pre/late-I neuron [10]. This drive signal consists of a tonic component and a concentration-dependent component. Its modulation by the chemical drive signal I_{ch} is described by,

$$I_i = c_i [1 + k_{ch,i} (I_{ch} - I_{ch0})] \quad (4)$$

where c_i is the nominal synaptic input to neuron i and I_{ch0} denotes the nominal chemical drive. The coefficient $k_{ch,i}$ characterizes the sensitivity of the synaptic input to changes in the chemical drive, I_{ch} .

The network tuning consists of two steps: First, for a given network structure, the connection matrix, the weights $\{c_i\}$ and the vagal feedback weights are determined such that a stable respiratory rhythm is obtained for the case of nominal chemical compositions. Note that due to the oscillatory nature of breathing there exist oscillations in the alveolar and arterial blood compositions [4] and, ultimately, in the chemical feedback signals [8], even under nominal conditions. Then, the coefficients $k_{ch,i}$ are tuned with

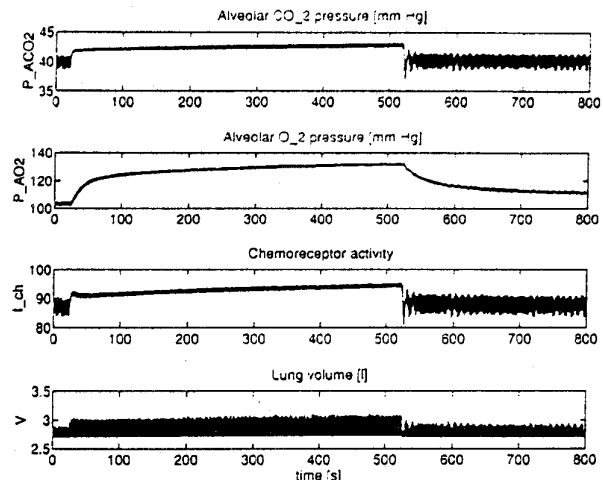


Figure 4: Model response to 5% CO_2 breathing.

the objective to reproduce experimentally observed closed-loop behaviors for a variety of physiological conditions. Figure 3 shows the nominal respiratory rhythm provided by the central pattern generator in the closed loop. In this figure, the neuron activities are represented by the numbers of spikes occurring within time periods of 0.1 s.

5. Simulation examples

Since the peripheral model provides realistic feedback to the respiratory network, a systematic validation of the network models and direct comparisons with experimental data are possible. Due to space limitations, only two cases are considered here:

Hypercapnia: Figure 4 shows the model response to 5% CO_2 breathing and its recovery from hypercapnia. In order to compensate partially for the increased CO_2 level, the central pattern generator increases both the frequency and the amplitude of its cycles, thereby increasing the ventilation rate. This behavior is consistent with experimental observations [3].

Hypoxia: The model behavior for low oxygen (9%) breathing and its recovery are shown in Figure 5. In sharp contrast to the rapid and monotonic decreases of both O_2 and CO_2 tensions on exposure to low oxygen air, periodic breathing occurred on re-exposure of the model to fresh air (21% O_2). Since the CO_2 concentration is comparatively small and the O_2 level rises fast after the latter transition, the chemical drive signal falls significantly and causes the respiratory pattern to cease temporarily, which in turn leads to an increase in the CO_2 level, a decrease in the O_2 level, and a reemergence of the respiratory

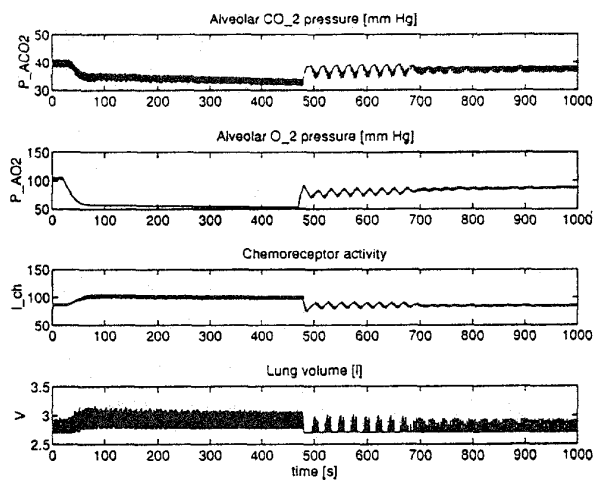


Figure 5: Model response to 9% O_2 breathing.

pattern. In agreement with clinical observations on periodic breathing [9], the severity of these oscillations in the simulations depended on (i) the sensitivity of the respiratory neurons to the chemical drive signal, k_{chi} , (i.e. the controller gain), and (ii) the arterial delay.

6. Conclusions

A closed-loop model of the respiratory control system that includes a neural network model of the central pattern generator has been developed. The model is capable of adjusting the breathing pattern in response to multiple feedback signals and has been shown to be consistent with experimental data under several physiological conditions, including hypoxia and hypercapnia.

References

- [1] S. M. Botros and E. N. Bruce, "Neural network implementation of a three-phase model of the respiratory rhythm generation," *Biol. Cybernetics*, **63**, 143–153, 1990.
- [2] G. W. Bradley, C. von Euler, I. Marttila and B. Roos, "A model of the central and reflex inhibition of inspiration in the cat," *Biol. Cybernetics*, **19**, 105–116, 1975.
- [3] F. J. Clark and C. von Euler, "On the regulation of depth and rate of breathing," *J. Physiol.*, **222**, 267–295, 1971.
- [4] F. L. Eldridge and D. E. Millhorn, "Oscillation, gating, and memory in the respiratory control system", In *Handbook of Physiology*, American Physiological Society, Bethesda, MD, 1986.
- [5] C. von Euler, "Brain stem mechanisms for generation and control of breathing pattern," In *Handbook of Physiology*, American Physiological Society, Bethesda, MD, 1986.
- [6] W. F. Fincham and F. T. Tehrani, "A mathematical model of the human respiratory system," *J. Biomed. Eng.*, **5**, 125–133, 1983.
- [7] W. F. Fincham and F. T. Tehrani, "On the regulation of cardiac output and cerebral blood flow," *J. Biomed. Eng.*, **5**, 73–75, 1983.
- [8] C. Gonzalez, L. Almara, A. Obeso and R. Rigual, "Carotid body chemoreceptors: From natural stimuli to sensory discharges," *Physiol. Rev.*, **74**, 829–898, 1994.
- [9] A. C. Guyton, *Textbook of Medical Physiology*, 8th Ed., Saunders, Philadelphia, 1991.
- [10] E. E. Lawson, D. W. Richter, D. Ballantyne and P. M. Lalley, "Peripheral chemoreceptor inputs to medullary inspiratory and postinspiratory neurons of cats," *Pflügers Archiv*, **414**, 523–533, 1989.
- [11] H. T. Milhorn, Jr., R. Benton, R. Ross and A. C. Guyton, "A mathematical model of the human respiratory control system," *Biophysical J.*, **5**, 27–46, 1965.
- [12] M. D. Ogilvie, A. Gottschalk, K. Anders, D. W. Richter and A. I. Pack, "A network model of respiratory rhythmicity," *Am. J. Physiol.*, **263**, R962–R975, 1992.
- [13] J. E. Remmers, D. W. Richter, D. Ballantyne, C. R. Bainton and J. P. Klein, "Reflex prolongation of stage I of expiration," *Pflügers Archiv*, **407**, 190–198, 1986.
- [14] I. A. Rybak and J. S. Schwaber, "Analysis of some neural network schemes for respiratory rhythmicity," Proc. World Congress on Neural Networks, San Diego, CA, vol. II, pages 744–749, 1994.
- [15] I. A. Rybak, J. F. R. Paton and J. S. Schwaber, "Modeling and analysis of some neural mechanisms for the genesis and control of respiratory pattern: 1. Models of single respiratory neurons," in preparation, 1995.

Appendix: Peripheral Model

The phrenic nerve activity, Ph , is considered the driving force for the respiratory periphery. The transformation of Ph into corresponding lung volume changes is assumed to be linear,

$$\tau_M \tau_L \ddot{\bar{V}} + (\tau_M + \tau_L) \dot{\bar{V}} + \bar{V} = K_m \bar{P}h \quad (5)$$

where $\bar{V} = V - V_0$ and $\bar{P}h = Ph - Ph_0$ are the lung volume and the phrenic nerve activity in the form of deviations from their respective resting levels, τ_M and τ_L are the time constants associated with muscles and lungs, respectively, and K_m is the gain of the phrenic to lung volume transfer function. Equation (5) constitutes the mechanical part of the periphery. The remaining parts of the respiratory periphery are modeled in terms of mass balances for the various compartments. Here we follow [6], taking into account the cyclic nature of breathing by using separate mass transfer equations for inspiration ($\dot{V} \geq 0$)

and expiration ($\dot{V} < 0$). Thus we obtain for the carbon dioxide and oxygen tensions in the alveolar space [6],

$$\frac{V}{P_b - 47} \frac{dP_{ACO_2}}{dt} + G_1 = (c_{VT_{CO_2}} - c_{aCO_2})Q_T + (c_{V_{BCO_2}} - c_{aCO_2})Q_B$$

$$\frac{V}{P_b - 47} \frac{dP_{AO_2}}{dt} + G_2 = (c_{V_{TO_2}} - c_{aO_2})Q_T + (c_{V_{BO_2}} - c_{aO_2})Q_B$$

where

$$\left. \begin{aligned} G_1 &= \frac{P_{ACO_2} - P_{ICO_2}}{P_b - 47} \dot{V} \\ G_2 &= \frac{P_{AO_2} - P_{IO_2}}{P_b - 47} \dot{V} \end{aligned} \right\} \text{ for } \dot{V} \geq 0$$

$$G_1 = G_2 = 0 \quad \text{for } \dot{V} < 0$$

The gas transfer within the lumped body tissue is modeled as follows:

$$S_T \frac{dc_{VT_{CO_2}}}{dt} = Q_T(c_{aCO_2} - c_{VT_{CO_2}}) + MR_{T_{CO_2}}$$

$$S_T \frac{dc_{V_{TO_2}}}{dt} = Q_T(c_{aO_2} - c_{V_{TO_2}}) - MR_{T_{O_2}}$$

Similarly, for the brain tissue,

$$S_B \frac{dc'_{V_{BCO_2}}}{dt} = Q_B(c'_{aCO_2} - c'_{V_{BCO_2}}) + MR_{B_{CO_2}}$$

$$S_B \frac{dc'_{V_{BO_2}}}{dt} = Q_B(c'_{aO_2} - c'_{V_{BO_2}}) - MR_{B_{O_2}}$$

where c'_{aCO_2} and c'_{aO_2} are delayed values of the arterial concentrations, $c'_{aCO_2}(t) = c_{aCO_2}(t - \theta)$, $c'_{aO_2}(t) = c_{aO_2}(t - \theta)$. It is assumed that the gas concentrations in the tissue are equal to those in venous blood. Furthermore, the alveolar and arterial CO_2 tensions are assumed equal, while the alveolar O_2 tension is 4 mm Hg higher than the arterial tension. The blood gas relationships are given next for CO_2 and O_2 , respectively:

$$c_{O_2} = K_1(1 - e^{-K_2 P_{O_2}})^2$$

$$c_{CO_2} = K_3 P_{CO_2}$$

The partial pressure of CO_2 at the site of the central receptors is assumed to be the CO_2 pressure at a depth, d , below the surface of the medulla, given by,

$$P_{cCO_2} = P_{V_{BCO_2}} + (P_{CSF_{CO_2}} - P_{V_{BCO_2}})e^{-d\sqrt{Q_B K_4}}$$

Finally, the diffusion of CO_2 across the blood-brain barrier is described by:

$$\frac{dP_{CSF_{CO_2}}}{dt} = \frac{1}{\tau_d} (P_{V_{BCO_2}} - P_{CSF_{CO_2}})$$

The model of the periphery also contains relationships for the tissue and brain blood flows, which are subject to regulation as well. These blood flows are primarily determined by local regulation of blood flow in the various tissue compartments; they can therefore be determined from metabolic rates in tissues as well as CO_2 and O_2 concentrations. Such relations for steady-state conditions are provided by [7]. They can be extended to match dynamic effects that have been observed experimentally by augmenting them with linear dynamic elements [6].

List of variables:

Symbol	Variable	Nominal Value
c	blood gas conc.	l/l
d	depth	0.015 cm
K_1	O_2 equil. const.	0.2
K_2	O_2 equil. const.	$0.046(mmHg)^{-1}$
K_3	CO_2 equil. const.	$0.016(mmHg)^{-1}$
K_4	central receptor const.	$346 \times 10^3 scm^{-2}l^{-1}$
$MR_{B_{CO_2}}$	metabolic rate	0.00091/s
$MR_{B_{O_2}}$	metabolic rate	0.0009251/s
$MR_{T_{CO_2}}$	metabolic rate	0.002871/s
$MR_{T_{O_2}}$	metabolic rate	0.003521/s
P	partial pressure	mm Hg
P_b	barometric pressure	760 mm Hg
P_{ICO_2}	CO_2 pressure	0 mm Hg
P_{IO_2}	O_2 pressure	149.7 mm Hg
Q_B	brain blood flow	0.01251/s
Q_T	tissue blood flow	0.070831/s
S_B	gas storage space	1.1l
S_T	gas storage space	50l
V_0	resting lung volume	2.7l
θ	arterial delay	10s
τ_d	diffusion time const.	320 s
τ_L	lung time constant	0.25s
τ_M	muscle time const.	0.25s

subscripts:

a	arterial
A	alveolar
B	brain
c	central receptor
CSF	cerebrospinal fluid
I	inspired air
T	tissue
v	venous